

## On the number of isolating integrals in Hamiltonian systems

George Contopoulos

*European Southern Observatory, Geneva, Switzerland*

Luigi Galgani and Antonio Giorgilli

*Istituto di Fisica e Istituto di Matematica dell'Università, Milano, Italy*

(Received 16 March 1978)

In a Hamiltonian system of three degrees of freedom we have found a large stochastic region (the "big sea"), some other stochastic regions, apparently separated from the above ("small seas"), and some ordered regions. In the ordered regions the maximal Lyapunov characteristic number vanishes, while it has finite values in the stochastic regions. However, these values are different in the big sea and the small seas. Three formal integrals were constructed and they were truncated at orders 2,3,...,11. The numerical values of the truncated integrals along several orbits were calculated. The variations of all three integrals decrease with order in the ordered region, while they remain large in the big sea. In a small sea two integrals have large relative variations, while one integral seems to be well conserved. This indicates that in the ordered region there are two integrals, in the big sea none, and in the small seas one integral beyond the energy.

### I. INTRODUCTION

The results of some numerical computations performed by Froeschlé and by Froeschlé and Scheidecker<sup>1</sup> led those authors to put forward the conjecture that in an autonomous Hamiltonian system with  $N$  degrees of freedom the number of isolating integrals apart from energy is either  $N - 1$  or zero. We performed some numerical computations on a particular model with  $N = 3$  degrees of freedom and found results which indicate that intermediate situations may appear in some cases.

Our model is described by the Hamiltonian

$$H = \sum_{i=1}^3 \frac{\omega_i}{2} (q_i^2 + p_i^2) + q_1^2 q_2 + q_2^2 q_3, \quad (1)$$

where

$$\omega_1 = 1, \quad \omega_2 = 1.4142, \quad \omega_3 = 1.7321. \quad (2)$$

The escape energy  $E_{\text{esc}}$ , i.e., the maximum value of the energy for which the energy surface has a compact component, is  $E_{\text{esc}} = 0.097$ .

Our calculations were made on the energy surface  $E = 0.09$ . We found a large stochastic region, which we call the "big sea." We found also other stochastic regions, which apparently are separated from the big sea and which we call "small seas." Finally, we also found some ordered regions.

The criterion discriminating between the stochastic and ordered regions is based on the maximal Lyapunov characteristic number,<sup>2</sup>  $\lambda_{\text{max}}$ , whose value is computed as described in Sec. II. If in a region  $\lambda_{\text{max}}$  is a positive constant, we say that this region is stochastic, while if  $\lambda_{\text{max}}$  vanishes we say that this region is ordered.

The formal integrals behave as constants in the

ordered region. Namely, if we truncate the series representing these integrals at a certain order we find some variation of the values of the truncated integrals along each orbit; if we truncate the integrals at a higher order the variation is smaller. By taking a sufficient number of terms one can make the variation of the (truncated) integral very small.<sup>3</sup>

On the other hand, in the large stochastic region we find large variations of the truncated integrals, and the situation is not improved by including higher-order terms. So the present calculations indicate that there is no integral of motion besides the energy in the big sea: the three formal integrals, calculated by the method described in Sec. III, are not at all constant.

However, in a small sea it has been found that one integral besides the energy is reasonably conserved, i.e., the variations of the integral truncated at successive orders are small.

### II. MAXIMAL LYAPUNOV CHARACTERISTIC NUMBER

Given a system of differential equations

$$\dot{x}_i = f_i(x_1, \dots, x_n), \quad i = 1, \dots, n, \quad (3)$$

and the corresponding variational system

$$\dot{\xi}_i = \sum_{k=1}^n \frac{\partial f_i}{\partial x_k}(x_1, \dots, x_n) \xi_k, \quad i = 1, \dots, n, \quad (4)$$

any set of initial data  $x_1^0, \dots, x_n^0, \xi_1^0, \dots, \xi_n^0$  gives a solution  $x_i(t; x_1^0, \dots, x_n^0), \xi_i(t; x_1^0, \dots, x_n^0, \xi_1^0, \dots, \xi_n^0)$ . It has been proven<sup>4</sup> that, if the system (3) is defined on a compact manifold and preserves a measure, as in our case, for almost all  $x_1^0, \dots, x_n^0$  and for all  $\xi_1^0, \dots, \xi_n^0$  the limit

$$\lim_{t \rightarrow \infty} \frac{1}{t} \ln \|\xi(t)\| = \lambda(x_1^0, \dots, x_n^0, \xi_1^0, \dots, \xi_n^0) \quad (5)$$

exists, where  $\|\xi(t)\|$  denotes the norm of  $\xi_1(t), \dots, \xi_n(t)$ . The quantities  $\lambda$  are called Lyapunov characteristic numbers. Given  $x_1^0, \dots, x_n^0$ ,  $\lambda$  takes at most  $n$  different values, and the maximum of them is denoted by  $\lambda_{\max}(x_1^0, \dots, x_n^0)$ . One can show<sup>2</sup> that, if one chooses  $\xi_1^0, \dots, \xi_n^0$  at random, with probability one, one obtains  $\lambda_{\max}$ . Moreover, being an integral of motion,  $\lambda_{\max}$  does not depend on the initial point  $x_1^0, \dots, x_n^0$  on an ergodic component.

For the technical computation of  $\lambda_{\max}$ , we integrated directly the system of equations (3) and (4) as given above. This method constitutes a technical improvement with respect to the one considered in Ref. 2, where  $\xi_i(t)$  was evaluated as  $x_i'(t) - x_i(t)$ , the difference between solutions of the system (3) corresponding to two sets of nearby initial data. We found that the present more direct method allows us to use integration steps much larger than the previous method. Moreover, it eliminates the technical problem of choosing a suitable initial distance between the nearby orbits.

### III. CONSTRUCTION OF THE INTEGRALS

If we have a Hamiltonian

$$H = H^{(2)}(q, p) + H^{(3)}(q, p) + \dots, \quad (6)$$

where

$$q = (q_1, \dots, q_n), \quad p = (p_1, \dots, p_n),$$

and

$$H^{(2)}(q, p) = \sum_{i=1}^n \frac{\omega_i}{2} (q_i^2 + p_i^2), \quad (7)$$

then we can construct  $n - r + 1$  formal independent integrals of motion if there are  $r$  independent resonance relations of the form

$$m_1 \omega_1 + \dots + m_n \omega_n = 0, \quad (8)$$

where  $m_i$  are integers not all vanishing; if  $r = 0$  we can construct  $n$  formal integrals of the form

$$\phi_i = \phi_i^{(2)} + \phi_i^{(3)} + \dots, \quad (9)$$

where

$$\phi_i^{(2)} = \frac{1}{2} \omega_i (q_i^2 + p_i^2) \quad (10)$$

are the harmonic energies.

The computer program that calculates these integrals is described in Ref. 5; it is based on a new algorithm<sup>6</sup> that gives at the same time the normal form of the Hamiltonian, and does not involve any inversion like the Birkhoff method. The program is also applicable in "near resonance" cases, and gives the appropriate forms of the

integrals in the neighborhood of each resonance.

In order to check this program we made the following comparisons with the results of some earlier calculations in systems of two degrees of freedom: (a) we compared the integrals given by this program with those found by a different method in some resonant cases<sup>3</sup>; (b) we compared the integral and the normal form in the case  $\omega_1 = \omega_2$  with those found by still another method by Gustavson<sup>7</sup>; (c) we compared the terms of fourth degree of the normal form with the analytic expression of Contopoulos and Hadjidemetriou<sup>8</sup>; and (d) we used the integral to derive the periodic orbits in some near-resonance cases studied by Contopoulos.<sup>9</sup>

In all cases we found complete agreement. In particular, in the last case we found much better agreement with the empirical periodic orbits by using higher-order terms of the integral.

The time needed to calculate the integrals and the normal form up to the terms of seventh order, in a system of two degrees of freedom, is 0.3 sec with the 7600 CDC computer of CERN. The analogous calculation with the program of Contopoulos<sup>3</sup> in the same computer needs 6.3 sec execution time. Thus the improvement is obvious.

The time needed to reach the eighteenth order is about 65 and 87 sec for the nonresonant and the resonant cases, respectively. In the case of three degrees of freedom the time needed to reach the eleventh degree terms is about 40 sec.

### IV. THE "BIG SEA" AND THE "SMALL SEAS"

The initial conditions were defined by assigning initial values to the harmonic energies with vanishing values for the coordinates  $q_1, q_2, q_3$ , i.e.,  $q_1 = q_2 = q_3 = 0$ ;  $p_i = (2E_i)^{1/2} / \omega_i$  ( $i = 1, 2, 3$ ), with given values for  $E_1, E_2, E_3$ . Nine typical initial conditions are given in Table I.

All the orbits were computed by a central-

TABLE I. The various orbits (1, ..., 9) considered in this paper.  $E_1, E_2, E_3$  are the values of the initial harmonic energies (with vanishing coordinates  $q_1, q_2, q_3$ ). The value of  $\lambda_{\max}$  is also given.

Orbit	$E_1$	$E_2$	$E_3$	$\lambda_{\max}$
1	0.0005	0.0895	0	0
2	0.005	0.085	0	0
3	0.0085	0.0815	0	$2 \times 10^{-3}$
4	0.009	0.081	0	$5 \times 10^{-3}$
5	0.025	0.065	0	$3 \times 10^{-2}$
6	0.020	0.070	0	$3 \times 10^{-2}$
7	0.09	0	0	$3 \times 10^{-2}$
8	0.01	0.01	0.07	$3 \times 10^{-2}$
9	0.03	0.03	0.03	$3 \times 10^{-2}$

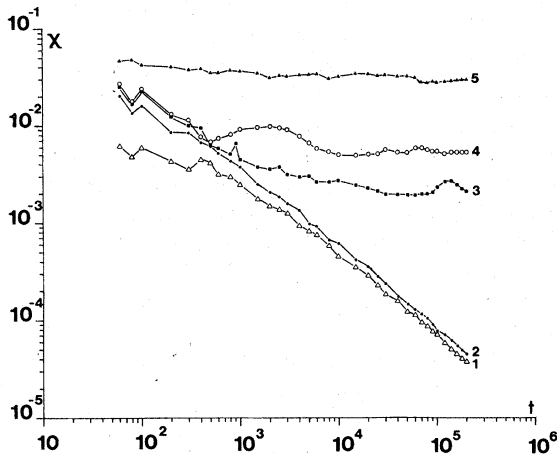


FIG. 1. Curves for  $\chi(t) = (1/t)\ln\|\xi(t)\|$  as a function of  $t$  in log-log scale for orbits 1-5 of Table I. By definition,  $\lambda_{\max} = \lim_{t \rightarrow \infty} \chi(t)$ .

point third-order method with a time step 0.05. Orbits 1-5 were computed up to time  $t = 2 \times 10^5$ , and 6-9 up to  $t = 5 \times 10^3$ .

The results for  $\chi(t) = (1/t)\ln\|\xi(t)\|$  as a function of  $t$  in log-log scale are reported in Fig. 1 for cases 1-5 and in Fig. 2 for cases 5-9. As one sees from Fig. 1 the orbits 1 and 2 give presumably vanishing values for  $\lambda_{\max} = \lim_{t \rightarrow \infty} \chi(t)$ , while orbits 3-5 give positive, rather well-stabilized values of  $\lambda_{\max}$ . These positive values are clearly different. On the other hand, in Fig. 2 all orbits give positive limiting values for  $\lambda_{\max}$ , which we consider to be the same as for orbit 5, namely,  $\lambda_{\max} \approx 0.03$ .

We interpret this situation as indicating that we are in presence of (a) an ordered region with  $\lambda_{\max} = 0$  (orbits 1, 2); (b) a large stochastic region with  $\lambda_{\max} \approx 0.03$  (the big sea; orbits 5-9); and (c) stochastic regions probably disjoint from the big sea (the small seas; orbits 3, 4 with  $\lambda_{\max} \approx 0.002$  and  $0.005$ , respectively).

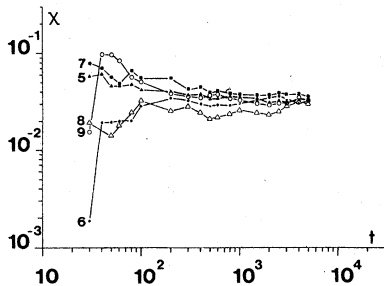


FIG. 2. The same as in Fig. 1 for orbits 5-9 of Table I. Orbits 6-9 have been computed for a much shorter time than orbit 5, but the tendency to a unique limit is clear by comparison with Fig. 1.

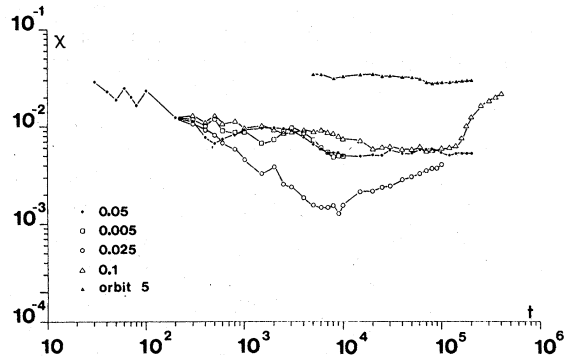


FIG. 3. Check of the stability of the results for  $\lambda_{\max} = \lim_{t \rightarrow \infty} \chi(t)$  with respect to changes in the integration step. The initial conditions are those of orbit 4, and the integration steps are from 0.005 to 0.1. For comparison's sake, the tail of the curve for orbit 5 is also reported.

In such a way we confirm a phenomenon already observed<sup>10</sup> for the case of five particles on a line with nearest-neighbor Lennard-Jones interaction.

It is of interest to check the stability of the results with respect to changes in the integration step. To this end let us consider a particularly critical case, i.e., that of a small sea, for example, orbit 4. In Fig. 3 four curves for  $\chi(t)$  are reported corresponding to four different steps and to the same initial conditions as orbit 4; the steps are 0.005, 0.025, 0.05 (orbit 4), 0.1, and the corresponding orbits were computed up to times  $10^4, 10^5, 2 \times 10^5, 4 \times 10^5$ , respectively. The curve corresponding to the big sea (orbit 5) is also reported for comparison's sake. As one sees, up to times  $10^5$  the agreement is quite good, namely, all curves appear to tend roughly to a unique value.

A particular discussion is required for the orbit

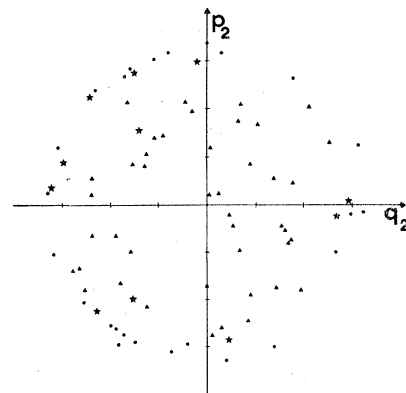


FIG. 4. Projections of the points of phase space on the plane  $(q_2, p_2)$  at times multiple of 5000 for orbit 4 with time step 0.1. Dots from 0 to  $1.2 \times 10^5$ , stars from  $1.2 \times 10^5$  to  $1.7 \times 10^5$ , triangles from  $1.7 \times 10^5$  to  $4 \times 10^5$ .

with time step 0.1. Up to time  $1.2 \times 10^5$  the agreement with the curve with time step 0.05 is quite good, while a striking feature appears after that time, namely,  $\chi(t)$  tends rather abruptly to the value of  $\lambda_{\max}$  for the big sea. In order to understand this fact it is of interest to have a picture of how the point moves with time in phase space. To this end the easiest thing to do is to plot at successive times the projections of such a point on the planes  $(q_1, p_1)$ ,  $(q_2, p_2)$ , and  $(q_3, p_3)$ . In Fig. 4 the projections at any time multiple of 5000 on the plane  $(q_2, p_2)$  are reported. From time 0 to time  $1.2 \times 10^5$  they are marked by dots, from  $1.2 \times 10^5$  to  $1.7 \times 10^5$  by stars, and from  $1.7 \times 10^5$  to  $4 \times 10^5$  by triangles. One sees that the harmonic energy of the second mode  $\frac{1}{2}\omega_2(p_2^2 + q_2^2)$  is well conserved up to  $t = 1.2 \times 10^5$ , while after that time such a quantity is no more conserved. This clearly means that the point moves after time  $1.2 \times 10^5$  in a region which is quite different from the region where it moved previously. As will be shown in Sec. V, the big sea is just characterized by nonconservation of the harmonic energy of the second mode. Analogous situations of changes of behavior were observed by us in the small sea in a few other cases; the phenomenon always disappeared by increasing the precision in the integration, i.e., the higher-precision calculations did not show a transition of the motion from the small sea to the big sea.

These are the facts. For what concerns the interpretation two possibilities are open: (i) the small seas are not disjoint from the big sea, but they communicate through small straits; (ii) the small seas and the big sea are disjoint and numerical errors cause the point to jump from a small sea into the big sea when the point happens to come sufficiently near the border.

### V. BEHAVIOR OF THE FORMAL INTEGRALS

Now we pass to discuss the formal integrals  $\phi_i$  ( $i = 1, 2, 3$ ) which were computed from order 2 to order 11.

Let us first show the behavior in the big sea and in a small sea. This is shown in Figs. 5 and 6 which refer to orbits 5 (big sea) and 4 (a small sea), respectively. In these figures we give the instantaneous values of the integrals  $\phi_1, \phi_2, \phi_3$  as functions of time for  $t$  multiple of 500 from 0 to 5000; the orders reported are 2 and 8 for the big sea and 2, 8, and 11 for the small sea. As the scale has been chosen to be logarithmic for the ordinates, small values for the integrals are particularly emphasized in our figures. Moreover, at orders greater than 2, negative values of the integrals are possible, which obviously could not be represented.

The three formal integrals have a very similar behavior in the big sea; they have large fluctuations, and no improvement appears if we go from the second-order integrals to the eighth-order integrals. In the small sea  $\phi_1$  and  $\phi_3$  have a behavior similar to that of the big sea. However, a different situation occurs for  $\phi_2$ . In fact  $\phi_2$  has rather small fluctuations which decrease from order 2 to order 8, and remain more or less of the same order of magnitude at order 11. For comparison's sake the fluctuations of the total energy in the latter computation, due to inaccuracies in the calculations, are from  $8.9962 \times 10^{-2}$  to  $9.0001 \times 10^{-2}$ , i.e., not visible in our scale.

Thus it appears that, in some sense, in the small sea we have one conserved integral besides the energy, notwithstanding the stochasticity of the system as proved by the positiveness of  $\lambda_{\max}$ .

This is indeed the main thesis of the present

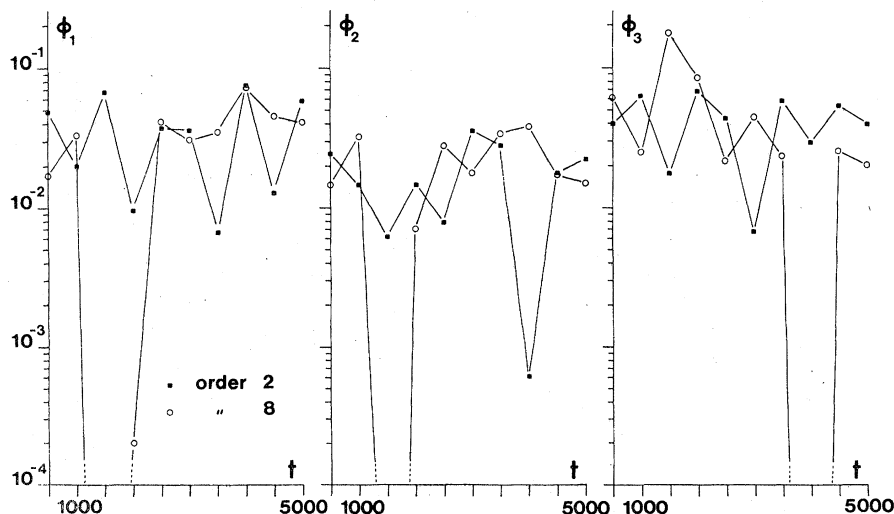


FIG. 5. Instantaneous values of the integrals  $\phi_1$ ,  $\phi_2$ , and  $\phi_3$  (left to right) truncated after the terms of order 2 (■) and 8 (○), at times multiple of 500 up to time 5000, for orbit 5 (big sea).

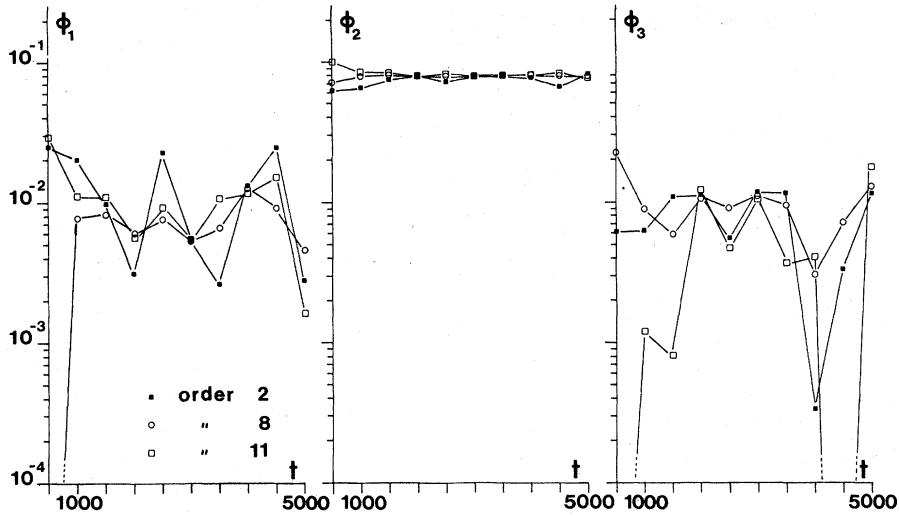


FIG. 6. Same as Fig. 5 for orbit 4 (small sea), plus the integrals truncated after the terms of order 11( $\square$ ).

work. So now we want to illustrate it in a somewhat different way, by showing the density of the probability distributions of the formal integrals at various orders. More precisely, we consider an interval  $(\phi^{\min}, \phi^{\max})$  in which the (truncated)

functions  $\phi_i$  can fluctuate, subdivide it into  $N$  equal subintervals, and count how many times a given function  $\phi_i$  (at a certain order) takes values in any subinterval up to a fixed time; the percentage is then plotted in a histogram.

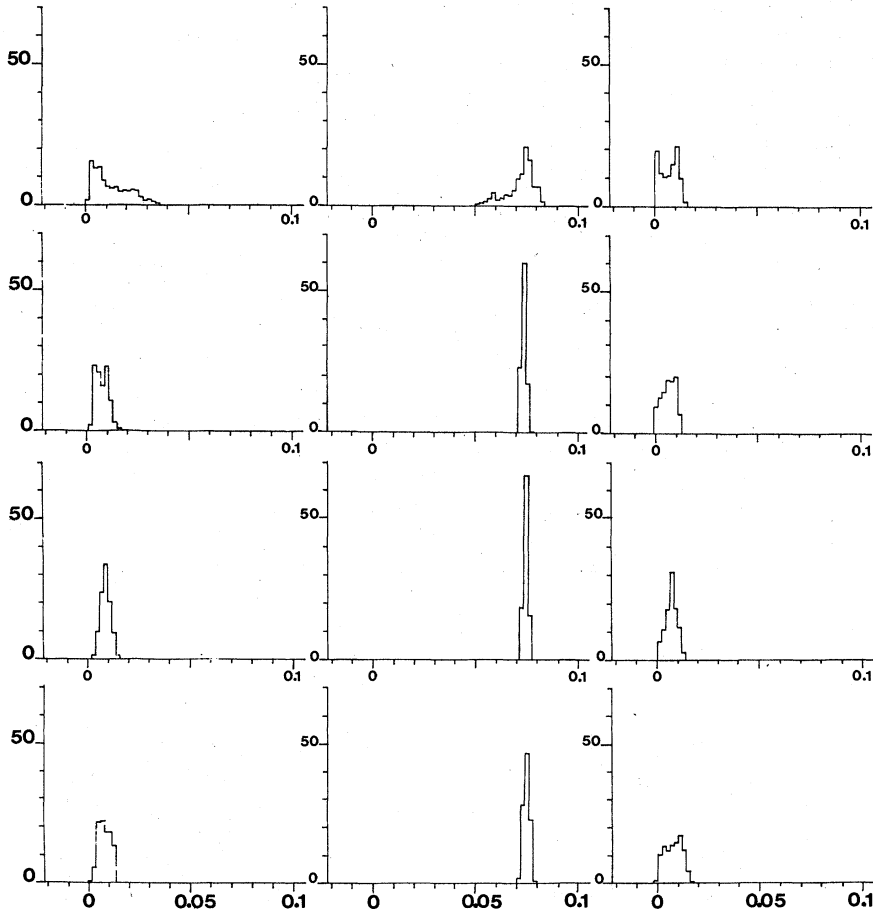


FIG. 7. Densities of probability distributions of  $\phi_1, \phi_2, \phi_3$  (left to right) at orders 2, 4, 6, 7 (from top) for orbit 4 (small sea).

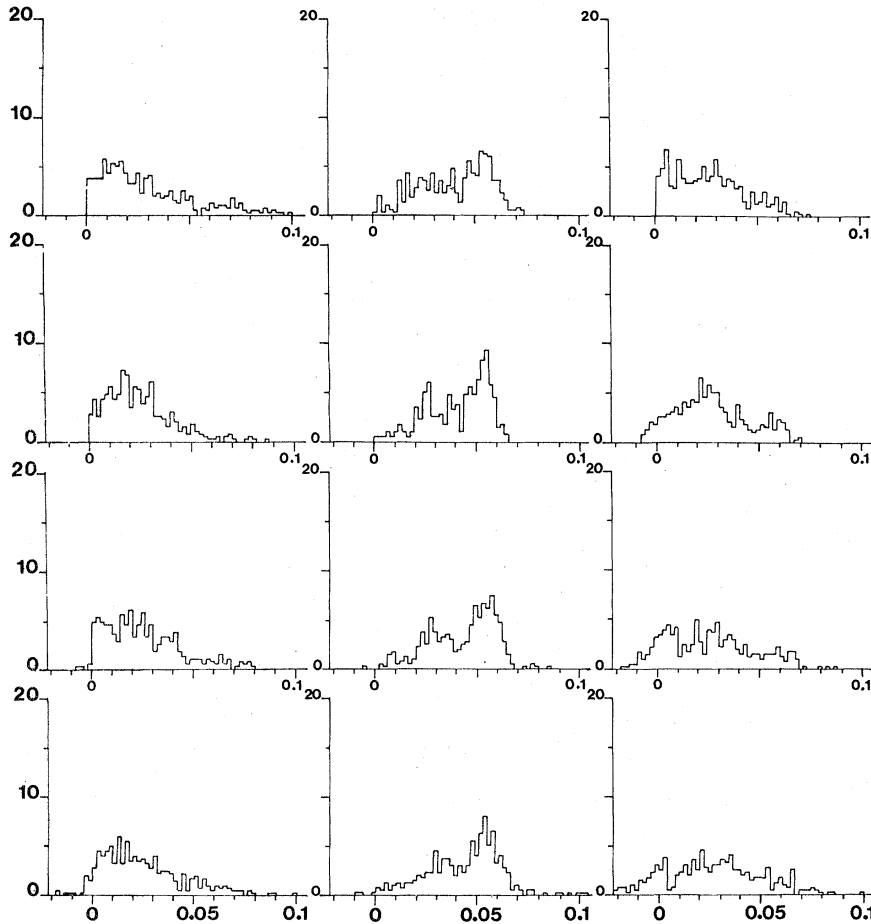


FIG. 8. Same as Fig. 7 for orbit 9 (big sea). Notice the change of scale for ordinates.

The histograms corresponding to the small sea (orbit 4) are reported in Fig. 7; here  $\phi^{\min} = -0.02$ ,  $\phi^{\max} = 0.1$ ,  $N = 60$ , and 500 points were considered at equal intervals of time up to  $t = 5000$ . The columns from left to right correspond to  $\phi_1$ ,  $\phi_2$ ,  $\phi_3$ , respectively, while the various rows correspond to orders 2, 4, 6, 7, from the top, respectively. The rather good "convergence" of the second integral  $\phi_2$  with respect to  $\phi_1$  and  $\phi_3$  is evident.

For comparison's sake we report the analogous histograms for the big sea (orbit 9) in Fig. 8.

The only difference with respect to Fig. 7 is in the scale of ordinates. As expected no indication of convergence is given. However, it is of interest to emphasize that these histograms confirm that the system is not ergodic on the energy surface considered. Indeed the three functions are not equally distributed; thus, for example, the average values at second order are 0.029, 0.039, and 0.026, respectively, and in general the histograms for  $\phi_2$  are particularly different from what one would expect in an ergodic case, as shown in Ref. 10.

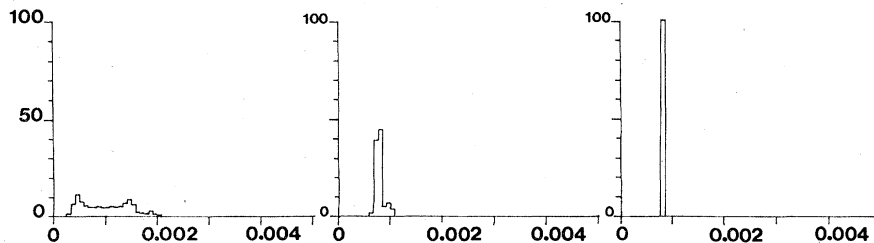


FIG. 9. Same as Fig. 7 for orbit 1 (ordered motion). The distributions are given only for  $\phi_1$  for orders 2, 4, and 7 (from left). Notice the change of scale for ordinates and abscissas.

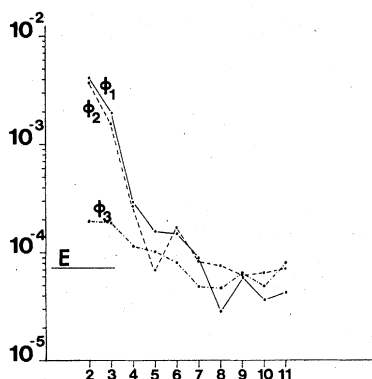


FIG. 10. Mean square deviations of  $\phi_1$ ,  $\phi_2$ ,  $\phi_3$  as functions of the order  $2, \dots, 11$  for orbit 1 (ordered motion). For comparison's sake, the mean-square deviation of the total energy, due to computational errors, is also given (straight line).

Finally, let us consider the case of an ordered motion, i.e., a case when  $\chi(t)$  appears to go to zero, so that one expects that the three integrals are well conserved. For example, we take orbit 1. Figure 9 gives histograms analogous to those of Figs. 7 and 8 for  $\phi_1$  at orders 2, 4, and 7 (from left). Here the scales of the ordinates and of the abscissas are changed;  $\phi^{\min} = 0.0$ ,  $\phi^{\max} = 0.005$ . The convergence is striking and the same happens

for  $\phi_2$  and  $\phi_3$ , the histograms of which are not reported here.

It is of interest to compare the fluctuations of these formal integrals at various orders with the fluctuation of the total energy  $E$  due to errors in computation, which are about  $7.4 \times 10^{-5}$  in the case of orbit 1 up to time 10 000. The comparison for orbit 1 is shown in Fig. 10, where the mean-square deviations of the integrals  $\phi_1, \phi_2, \phi_3$ , computed over a time from 0 to 10 000, as functions of the order  $k=2, \dots, 11$  are given. The mean-square deviation of energy is also indicated by a straight line. As one sees, the curves give an excellent indication of convergence up to the threshold afforded by the energy conservation.

## VI. CONCLUSION

As a conclusion we may consider our numerical computations as suggesting that the number of well-conserved integrals is, apart from total energy, 2 in the ordered region, 0 in the big sea, and possibly 1 in the small seas. Actually, in the case of the small seas, we can only say that the region which defines them in phase space can be rather well described in terms of such formal integrals. However, the problem of whether these regions are really disjoint from the big sea has to be considered as open.

<sup>1</sup>C. Froeschlé, *Astrophys. Space Sci.* **14**, 110 (1971); C. Froeschlé and J. P. Scheidecker, *ibid.* **25**, 373 (1973).

<sup>2</sup>G. Benettin, L. Galgani, and J.-M. Strelcyn, *Phys. Rev. A* **14**, 2338 (1976).

<sup>3</sup>G. Contopoulos, *Astrophys. J. Suppl.* **13**, 503 (1966).

<sup>4</sup>V. I. Oseledec, *Trans. Moscow Math. Soc.* **19**, 197 (1968).

<sup>5</sup>A. Giorgilli, *Comp. Phys. Commun.* (to be published).

<sup>6</sup>A. Giorgilli and L. Galgani, *Celest. Mech.* (to be published).

<sup>7</sup>F. G. Gustavson, *Astron. J.* **71**, 670 (1966).

<sup>8</sup>G. Contopoulos and J. Hadjidemetriou, *Astron. J.* **73**, 86 (1968).

<sup>9</sup>G. Contopoulos, *Astrophys. J.* **153**, 83 (1968).

<sup>10</sup>M. C. Carotta, C. Ferrario, G. Lo Vecchio, and L. Galgani, *Phys. Rev. A* **17**, 786 (1978).